Acta Crystallographica Section A
Foundations of Crystallography
ISSN 0108-7673

Received 4 November 2009
Accepted 4 July 2010

Polarization effects and phase equilibria in high-energy-density polyvinylidene-fluoride-based polymers

V. Ranjan,[a] L. Yu,[a] Serge Nakhmanson,[b] Jerry Bernholc[a,c] and M. Buongiorno Nardelli[a,c]*

[a]Center for High Performance Simulation and Department of Physics, North Carolina State University, Raleigh, NC 27695-7518, USA, [b]Materials Science Division, Argonne National Laboratory, Argonne, IL 60439, USA, and [c]Computer Science and Mathematics Division, Oak Ridge National Laboratory, Oak Ridge, TN 37831-6367, USA. Correspondence e-mail: mbnardelli@ncsu.edu

Using first-principles calculations, the phase diagrams of polyvinylidene fluoride (PVDF) and its copolymers under an applied electric field are studied and phase transitions between their nonpolar α and polar β phases are discussed. The results show that the degree of copolymerization is a crucial parameter controlling the structural phase transition. In particular, for tetrafluoroethylene (TeFE) concentration above 12%, PVDF–TeFE is stabilized in the β phase, whereas the α phase is stable for lower concentrations. As larger electric fields are applied, domains with smaller concentrations ($\leq$ 12%) undergo a transition from the α to the β phase until a breakdown field of ~600 MV m^{-1} is reached. These structural phase transitions can be exploited for efficient storage of electrical energy.

1. Introduction

Dielectric materials are regularly used for storing energy and play an important role in electric power systems. Since polymers constitute an important class of dielectrics, there is tremendous interest in research on polymers for future energy-storage media. The most commonly used dielectric polymer, polypropylene, has an energy density of 4 J cm^{-3}. However, the energy density in this material is largely due to its high breakdown field, because its dielectric constant is small. Here we report on a novel mechanism for storing high energy in a well known ferroelectric polymer: polyvinylidene fluoride (PVDF). PVDF and its copolymers exhibit excellent electromechanical properties and have great potential as future electrical storage media. In general, polymers have several advantages over currently used materials for energy storage, such as high electric breakdown field, low dielectric loss, fast charge–discharge speed, low cost and high reliability.

Among polymers, PVDF exhibits interesting electrical properties which are related to its crystal structure. It is most commonly found in a nonpolar α phase. It also exists in polar phases, such as β, γ and δ. Among these, the β phase is the one that has the highest polarization and will be the subject of this study.

In this paper we will discuss the phase diagram of a particular copolymer, polyvinylidene fluoride–tetrafluoroethylene, P(VDF–TeFE). The paper is organized as follows: the morphology of the copolymer is discussed in §1. §2 summarizes the methodological techniques used in the calculations. The results are discussed in §3, while §4 contains our conclusions.

2. Morphology

The structure of PVDF is summarized in Fig. 1. A single chain of PVDF is found in a *trans-gauche-trans-gauche′* (TGTG′) conformation in the α phase of PVDF and in all-*trans* (TT) conformations in the β phase. A *trans* (T) designation denotes a dihedral angle of 180°, whereas G and G′ imply dihedral angles of ~57° and ~−57°, respectively, obtained in our first-principles calculations. At low copolymer concentrations, the TGTG′ conformation is the most stable. The chains organize themselves in an antipolar arrangement within the unit cell in α-PVDF and in a polar arrangement in β-PVDF (Fig. 2). The α phase belongs to the space group $P2_1/c$ (C_{2h}^5). The β phase belongs to the space group $Amm2$ (C_{2v}^{14}). The α phase has the lowest total energy (Ranjan *et al.*, 2007; Su *et al.*, 2004). However, in copolymers of VDF and trifluoroethylene (TrFE[$-CF_2-CHF-$]) with about 50–80% VDF, the β phase is formed directly and a ferroelectric phase transition has been observed below the melting point (Samara, 2001).

3. Methodology

Electronic structure and total energy calculations have been performed using density-functional theory (DFT) (Hohenberg & Kohn, 1964; Kohn & Sham, 1965) with Vanderbilt ultrasoft

doi:10.1107/S0108767310026358

pseudopotentials (Vanderbilt, 1990) and a Perdew–Burke–Ernzerhof (PBE) exchange-correlation functional (Perdew *et al.*, 1996), as implemented within the *quantum-ESPRESSO* package (Giannozzi *et al.*, 2009). We chose a cutoff energy of 35 Rydberg and a Monkhorst–Pack (MP) (Monkhorst & Pack, 1976) k-point grid of $2 \times 4 \times 4$ for well converged results in both the α and β structures. In the relaxation process the forces are converged to less than 0.05 eV Å^{-1} and stresses to less than 0.05 GPa. The effect of the electric field is introduced following Fu & Bellaiche (2003), *i.e.* the total force is calculated by adding a term $eZ_i^{\star}E$ to the Hellman–Feynman forces $\mathbf{f}_i$, where $Z_i^{\star}$ are the Born effective charges for each atom and e is the elementary charge. The atomic structure is relaxed until the total force on each atom is close to zero, *i.e.* until $\mathbf{f}_i = -eZ_i^{\star}E$. The Born effective charges $Z_i^{\star}$ for each of the ions i are evaluated using density-functional perturbation theory (Sai *et al.*, 2002; Fu & Bellaiche, 2003; Antons *et al.*, 2005).

The equilibrium structure of PVDF under an electric field is obtained by minimizing the electric enthalpy F per unit cell,

$$F(E) = E_{\rm KS} - \Omega \mathbf{P} \cdot \mathbf{E}, \qquad (1)$$

where $E_{\rm KS}$ is the internal energy obtained from the Kohn–Sham functional and $\mathbf{P} = \mathbf{P}_{\rm ion} + \mathbf{P}_{\rm el}$ is the total (ionic plus electronic) macroscopic polarization, obtained using the Berry phase approach (King-Smith & Vanderbilt, 1993). Within this scheme, the field dependences of $\mathbf{f}_i$ and $Z_i^{\star}$ are neglected, because they are computed at $E = 0$. Therefore, the field only enters explicitly as a multiplier of $Z_i^{\star}$ and the results are rigorously correct only to first order in the field (Antons *et al.*, 2005).

4. Results

The polarization of β-PVDF has been calculated using various theoretical models proposed in the last three decades. In an extensive review, Kepler & Anderson (1992) described the polarization calculations using a rigid-dipole model and various methods to add corrections to it. Mopsik and Broadhurst treated PVDF as an electret and calculated polarization using the Onsager cavity approach (Mopsik & Broadhurst, 1975), whereas Tashiro *et al.* calculated polarization using a point-charge model (Tashiro *et al.*, 1980). We have summarized these results and compared them to our own calculations (Nakhmanson *et al.*, 2004, 2005) in Table 1.

One caveat in interpreting these results is that β-PVDF typically used in experiments displays a very low degree of crystallinity. We therefore see a big difference between our *ab initio* calculations of polarization in β-PVDF and the experimentally reported values. However, copolymers of PVDF can be grown 80 to 90% crystalline. Hence, we calculated polarization for P(VDF–TrFE)[P(VDF–TeFE)] with varying TrFE [TeFE] concentrations and interpolated values of $P_3^{\rm sp}$ for TrFE and TeFE copolymers over the entire range from 0 to 100% (Nakhmanson *et al.*, 2005). They compare very well with the experimentally reported data (Tajitsu *et al.*, 1987; Tasaka & Miyata, 1985) for concentrations larger than 20%.

Table 1
The polarization $P_3^{\rm sp}$ (C m^{-2}) in β-PVDF obtained using various theoretical models and measured experimentally.

Our first-principles calculations (Nakhmanson *et al.*, 2004) produce results that differ significantly from the experimental ones. This is primarily because we assume 100% crystallinity in our calculations, whereas experimental samples consist of ~60% crystalline β-PVDF.

Reference	Year	$P_3^{\rm sp}$
Kepler & Anderson (1992)		0.131
Mopsik & Broadhurst (1975)	1970–1975	0.22
Tashiro *et al.* (1980)	1980	0.140
Carbeck *et al.* (1995), Carbeck & Rutledge (1995)	1995	0.182
Nakhmanson *et al.* (2004)	2005	0.178
Experiment (Sawai *et al.*, 2003)		0.05

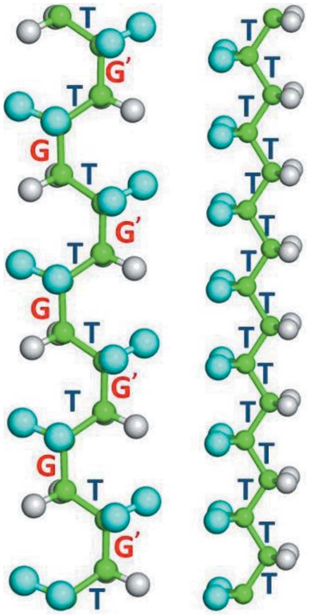

Figure 1
A single PVDF chain in TGTG′ (left) and all-*trans* (right) configurations.

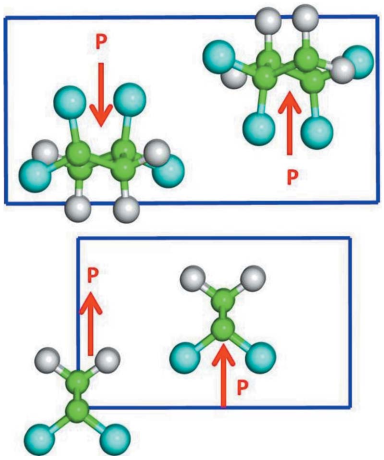

Figure 2
The unit cell of bulk PVDF in the α (top) and β (bottom) phases. The α phase is antipolar, since the dipoles in the alternate chains cancel, while in the β phase they are parallel to each other.

Next, we calculated the total energy of the α and β phases of PVDF. The total energy of α-PVDF is 23 meV per carbon atom lower than that of β-PVDF. Hence, α is the low-temperature stable phase of this polymer, in agreement with earlier investigations (Samara, 2001; Su *et al.*, 2004). The Born effective charges for each atom are obtained from the zero-field ground-state structures of α- and β-PVDF. Both phases were then subjected to electric fields and their free energies were minimized following the scheme described above.

In Fig. 3(*a*) we report the change in the free energy for both phases as the electric field is varied from 0 to 1000 MV m^{-1}. Owing to negligible polarization in the α phase, its free energy remains approximately constant over the entire field range. In contrast, the free energy of the polar β phase decreases with the field and β becomes the stable phase at fields above ~800 MV m^{-1}. The calculated critical field is similar to the ones reported in the literature, where it is usually quoted as ~500 MV m^{-1} (Davis *et al.*, 1978). Fig. 3(*b*) shows the electric displacement $D = E + 4\pi P$ as a function of the applied electric field for both α and β phases. The displacement field changes relatively little with the field in each phase, but the change in the stable phase at the critical field of ~800 MV m^{-1} results in a large discontinuous change in D. The vertical line marks the transformation from the α to the β phase. The volume change at the transition is discontinuous, 4.5%, which is a signature of a first-order phase transition. Therefore, nucleation of the β phase is required at the transition.

Our previous total-energy calculations (Ranjan *et al.*, 2007) show that the ground state of PVDF at zero temperature is a nonpolar phase with zero net polarization (α phase). However, various reports state that the polar β phase can be stabilized if PVDF is co-polymerized with some ‘impurity’ monomers. Nevertheless, even the polar PVDF cannot store a very large energy density as its polarization saturates at a relatively small electric field (Ranjan *et al.*, 2007). Instead, we have recently proposed a mechanism that explains the observed (Chu *et al.*, 2006) extraordinarily high energy density in P(VDF–CTFE) polymers (where CTFE chlorotrifluoroethylene) as due to electric-field-induced phase transformation from the α to the β phase. Furthermore, we showed (Ranjan *et al.*, 2007) that the β phase of P(VDF–CTFE) becomes more energetically favorable with increasing CTFE concentration, and becomes the ground state for a CTFE concentration greater than ~17%. This assignment is in agreement with X-ray data for the initial phase of P(VDF–CTFE). The gradual increase in the energy density and the nonlinear increase in the displacement field were attributed to the presence of nanodomains with different concentrations of CTFE and thus different critical fields needed to induce the transition in each domain. Furthermore, we have shown that by varying the composition and the disorder, the energy density could be improved further, up to 25–30 J cm^{-3}.

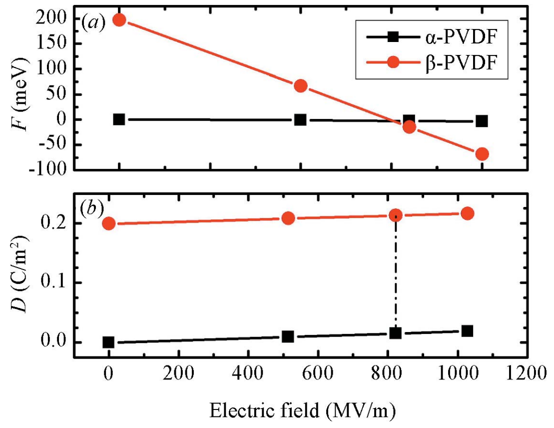

Figure 3
(*a*) Free energy of α- and β-PVDF under an external electric field. The nonpolar α-PVDF phase has a lower free energy below ~800 MV m^{-1}. At higher fields the β phase is energetically favored. (*b*) The electric displacement changes discontinuously at the transition from the α to the β phase.

We are now extending this investigation to the more common copolymers of VDF, to see whether they can be used in high-energy-density applications and, if so, to identify and optimize their composition ranges. Here, we present our finding for P(VDF–TeFE). The copolymers are built on simple atomic substitutions in the basic VDF repeat unit. The VDF repeat unit consists of a C—C bond, where two F atoms are attached to one C atom and two H atoms are attached to the other. The CTFE unit is created when one of the H atoms is replaced by F and the other by Cl in the VDF monomer. TeFE, a much more common copolymer than VDF, is obtained if both H atoms in the VDF unit are replaced by F.

The results of our total energy calculations are summarized in Fig. 4, where we show the energy difference (per carbon atom) between the α and β phases of PVDF–TeFE as a function of TeFE concentration. In the limit of pure PVDF (TeFE concentration = 0), the α phase is lower in energy and hence is the stable phase. The transition from the α to the β phase takes place at 12% TeFE concentration. In an earlier calculation (Ranjan *et al.*, 2007) we have shown that a CTFE concentration of 17% leads to a transition from the α to the β phase in P(VDF–CTFE). These differences between the TeFE- and CTFE-substituted PVDF lead to small changes in the overall results.

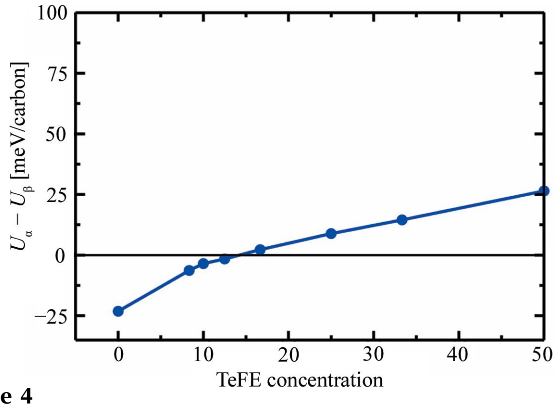

Figure 4
Calculated total energy difference between the α and β phases, divided by the number of carbon atoms in the unit cell, as a function of TeFE concentration (in %) in PVDF–TeFE.

It can be noted that in general one needs a smaller electric field for the α–β conversion in P(VDF–TeFE) than in P(VDF–CTFE). Furthermore, for exactly the same sample with CTFE replaced by TeFE, P(VDF–TeFE) will have a larger displacement field D at a given applied electric field E. This is due to the earlier onset of the transition in P(VDF–TeFE), as well as the shape of the displacement *versus* concentration curve. However, this information alone is not enough to estimate the energy density of the polymer, since concentration and disorder both play major roles.

To introduce the effect of disorder we have used a model in which we assume that a disordered P(VDF–CTFE) or P(VDF–TeFE) sample consists of ‘nanodomains’, each with a slightly different concentration of CTFE or TeFE. Taking a Gaussian distribution of these domains, the probability $n(x)$ of a domain with concentration x% and disorder σ becomes

$$n(x) = \frac{1}{(2\sigma\pi)^{1/2}} \exp\left[-\frac{(x-x_0)^2}{2\sigma^2}\right]. \qquad (2)$$

The contribution to the polarization of the domains that remain in the α phase turns out to be small enough that it can be neglected. The total polarization at a given field is then given by

$$P(E) = \int_0^1 \mathrm{d}x \int_0^E \mathrm{d}E'\, P_\beta(x)\, n(x)\, \delta[E' - E_{\rm crit}(x)], \qquad (3)$$

where $n(x)$ is the normalized probability of having a domain with concentration x. The resulting displacement field $D = E + 4\pi P$ as a function of the applied field E is depicted in Fig. 5. We are not aware of any experimental results for P(VDF–TeFE) in these ranges. Hence, we have tried out various scenarios with varying average impurity concentration x_0 and the sample disorder parameter σ. When the impurity concentration is 10%, D saturates at smaller E for a sample with σ = 3% (green curve), as compared to one with σ = 5% (red curve). However, when x_0 is reduced to 5%, D does not saturate even at a much higher electric field. For comparison, we have also plotted the curve for P(VDF–CTFE) with x_0 = 10% and σ = 5%. P(VDF–TeFE) with x_0 = 5% compares well with this PVDF–CTFE configuration.

Next, we plot the calculated energy density in Fig. 6 for all the cases presented in Fig. 5. This density is defined as $\xi = \int E\,\mathrm{d}D$, where E is the applied electric field and D is the electric displacement. As can be seen in the figure, the P(VDF–TeFE) sample with x = 10% has a smaller energy density than the corresponding P(VDF–CTFE) sample. However, the P(VDF–TeFE) sample with x = 5% and σ = 3% exhibits a slightly better ‘theoretical’ energy storage capacity than the P(VDF–CTFE) sample with x = 10%. The difference is due to a reduced percentage of the impurity monomer, which results in greater energy change after the phase transition, because the critical field decreases with impurity concentration.

However, kinetic effects are completely left out by the above energy-only considerations. Under actual capacitor operations, the sample must have enough kinetic freedom to transform from one phase to the other as the electric field is increased and then released. The CTFE units, by being bulkier than TeFE, increase the volume of the polymer and therefore may provide more kinetic freedom for the transformation. Alternatively, careful nano-structuring and/or a filler material may facilitate the kinetics. Nevertheless, while our investigations are still ongoing, it is already clear that the phase-transformation route we have elucidated provides several avenues for material optimization in the quest for high-energy storage materials.

5. Conclusion

In conclusion, we have shown that an electric-field-induced phase transition in copolymers of PVDF can result in a highly increased energy storage capacity. The presence of copolymers in different concentrations helps to control the phase transition from a nonpolar to a polar structure, which is responsible for the high-density storage of electrical energy. Furthermore,

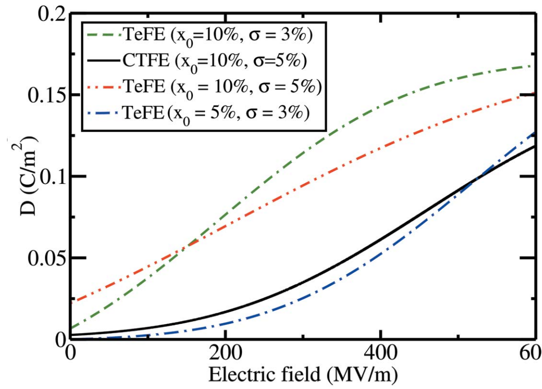

Figure 5
The electric displacement as a function of the electric field for P(VDF–TeFE) with different x_0 and σ. For comparison, one such scenario is also presented for PVDF–CTFE. D saturates at a much lower electric field for PVDF–TeFE as compared to PVDF–CTFE. However, when x_0 is smaller TeFE and CTFE compare well with each other.

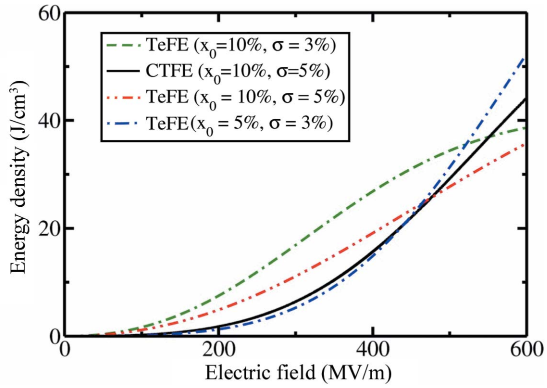

Figure 6
Energy storage density for PVDF–TeFE and PVDF–CTFE for the same concentrations as presented in Fig. 5. The energy densities of the two materials are comparable when the TeFE concentration is much smaller than that of CTFE.

disorder effects lead to an enhanced energy density and help explain recent experimental results.

This work was supported by the Office of Naval Research. The calculations were carried out at the NCCS-ORNL. SN was supported by BES, US DOE, under contract No. DE-AC02-06CH11357. MBN acknowledges partial support of BES, US DOE at ORNL (DE-FG02-98ER14847 and DE-AC05-00OR22725 with UT-Batelle, LLC).

References

Antons, A., Neaton, J. B., Rabe, K. M. & Vanderbilt, D. (2005). *Phys. Rev. B*, **71**, 024102.

Carbeck, J. D., Lacks, D. J. & Rutledge, G. C. (1995). *J. Chem. Phys.* **103**, 10347–10355.

Carbeck, J. D. & Rutledge, G. C. (1995). *Polymer*, **37**, 5089–5097.

Chu, B., Zhou, X., Ren, K., Neese, B., Lin, M., Wang, Q., Bauer, F. & Zhang, Q. M. (2006). *Science*, **313**, 334–336.

Davis, G. T., McKinney, J. E., Broadhurst, M. G. & Roth, S. C. (1978). *J. Appl. Phys.* **49**, 4998–5002.

Fu, H. & Bellaiche, L. (2003). *Phys. Rev. Lett.* **91**, 057601.

Giannozzi, P. *et al.* (2009). *J. Phys. Condens. Matter*, **21**, 395502.

Hohenberg, P. & Kohn, W. (1964). *Phys. Rev. B*, **136**, 864–871.

Kepler, R. G. & Anderson, R. A. (1992). *Adv. Phys.* **41**, 1–57.

King-Smith, R. D. & Vanderbilt, D. (1993). *Phys. Rev. B*, **47**, 1651–1654.

Kohn, W. & Sham, L. J. (1965). *Phys. Rev. A*, **140**, 1133–1138.

Monkhorst, H. J. & Pack, J. D. (1976). *Phys. Rev. B*, **13**, 5188–5192.

Mopsik, F. & Broadhurst, M. G. (1975). *J. Appl. Phys.* **46**, 4204–4208.

Nakhmanson, S. M., Buongiorno-Nardelli, M. & Bernholc, J. (2004). *Phys. Rev. Lett.* **92**, 115504.

Nakhmanson, S. M., Buongiorno-Nardelli, M. & Bernholc, J. (2005). *Phys. Rev. B*, **72**, 115210.

Perdew, J. P., Burke, K. & Ernzerhof, M. (1996). *Phys. Rev. Lett.* **77**, 3865–3868.

Ranjan, V., Yu, L., Buongiorno-Nardelli, M. & Bernholc, J. (2007). *Phys. Rev. Lett.* **99**, 047801.

Sai, N., Rabe, K. M. & Vanderbilt, D. (2002). *Phys. Rev. B*, **66**, 104108.

Samara, G. A. (2001). *Solid State Physics*, edited by H. Ehrenreich & F. Spaepen, Vol. 56, pp. 240–458. San Diego, San Francisco, New York, Boston, London, Sydney, Tokyo: Academic Press.

Sawai, D., Watanabe, Y., Taguchi, D., Takahashi, Y., Furukawa, T. & Kanamoto, T. (2003). *J. Polym. Sci. B Polym. Phys.* **41**, 1701–1712.

Su, H., Strachan, A. & Goddard III, W. A. (2004). *Phys. Rev. B*, **70**, 064101.

Tajitsu, Y., Ogura, H., Chiba, A. & Furukawa, T. (1987). *Jpn. J. Appl. Phys.* **26**, 554–560.

Tasaka, S. & Miyata, S. (1985). *J. Appl. Phys.* **57**, 906–910.

Tashiro, K., Kobayashi, M., Tadokoro, H. & Fukada, E. (1980). *Macromolecules*, **13**, 691–698.

Vanderbilt, D. (1990). *Phys. Rev. B*, **41**, 7892–7895.